MCNPX Simulation of Proton Dose Distributions in a Water Phantom

Chung-Chi Lee[1,2,3], Yun-Jing Lee[4], Shih-Kuan Chen[1], Bing-Hao Chiang[1], Chuan-Jong Tung[1,3], Tsi-Chian Chao[1,3]

Background: This study presents the Monte Carlo N-Particles Transport Code, Extension (MCNPX) simulation of proton dose distributions in a water phantom.

Methods: In this study, fluence and dose distributions from an incident proton pencil beam were calculated as a function of depth in a water phantom. Moreover, lateral dose distributions were also studied to understand the deviation among different MC simulations and the pencil beam algorithm. MCNPX codes were used to model the transport and interactions of particles in the water phantom using its built-in "repeated structures" feature. Mesh Tally was used in which the track lengths were distributed in a defined cell and then converted into doses and fluences. Two different scenarios were studied including a proton equilibrium case and a proton disequilibrium case.

Results: For the proton equilibrium case, proton fluence and dose in depths beyond the Bragg peak were slightly perturbed by the choice of the simulated particle types. The dose from secondary particles was about three orders smaller, but its simulation consumed significant computing time. This suggests that the simulation of secondary particles may only be necessary for radiation safety issues for proton therapy. For the proton disequilibrium case, the impacts of different multiple Coulomb scattering (MCS) models were studied. Depth dose distributions of a 70 MeV proton pencil beam in a water phantom obtained from MCNPX, Geometry and Track, version 4, and the pencil beam algorithm showed significant deviations between each other, because of different MCS models used.

Conclusions: Careful modelling of MCS is necessary when proton disequilibrium exists.
(Biomed J 2015;38:414-420)

At a Glance Commentary

Scientific background of the subject

MCNPX has been used in this paper to simulate the patient doses of proton therapy. In the case of proton equilibrium, particle fluences and doses before and after the Bragg peak were studied. Proton dose distributions for different multiple Coulomb scattering models have also been studied for proton equilibrium cases.

What this study adds to the field

The sub-centimetre lateral dose distribution was significantly deviated owing to proton disequilibrium and multiple scattering, predominantly because the FWHM of proton scattering inside water is in the order of millimeter, which may clarify dose distribution under proton disequilibrium, which is likely to occur in lung dosimetry.

Key words: Monte Carlo simulation, multiple Coulomb scattering, pencil beam algorithm, proton disequilibrium, proton therapy

Proton therapy has gained wide interest in recent years as it can deliver most of the radiation dose to the tumor while sparing the normal tissues. This is clearly demonstrated by the increasing number of patients treated using such a state-of-the-art modality. As of May 2015, there are 58 particle facilities in operation, 36 facilities

From the [1]Department of Medical Imaging and Radiological Sciences, College of Medicine, Chang Gung University, Taoyuan, Taiwan; [2]Department of Radiation Oncology, Chang Gung Memorial Hospital at Linkou, Chang Gung University College of Medicine, Taoyuan, Taiwan; [3]Medical Physics Research Center, Institute for Radiological Research, Chang Gung Memorial Hospital at Linkou/Chang Gung University College of Medicine, Taoyuan, Taiwan; [4]Department of Radiation Oncology, Ministry of Health and Welfare Nantou Hospital, Nantou, Taiwan

Received: Jun. 23, 2014; Accepted: Sep. 15, 2015

Correspondence to: Dr. Tsi-Chian Chao, Department of Medical Imaging and Radiological Sciences, College of Medicine, Chang Gung University, Taoyuan, Taiwan. 259, Wenhua 1st Rd., Gueishan, Taoyuan 333, Taiwan (ROC). Tel.: 886-3-2118800 ext. 5385; Fax: 886-3-2118700; E-mail: chaot@mail.cgu.edu.tw

DOI: 10.4103/2319-4170.167078

under construction, and more than 100,000 patients treated worldwide.[1] In Taiwan, Chang Gung Memorial Hospital (CGMH) in Linkou will officially accpet patients in late 2015. In addition, four other proton/heavy ion centres are currently in planning. These facilities are the most advanced cancer treatment modality in radiotherapy, which requires state-of-the-art techniques to perform dosimetry.

Patient dose simulation for proton therapy demands an algorithm that is not only capable of accurate beamline modelling, but also possesses the ability to process complex patient tissue composition that is often obtained from the patient's computed tomography (CT) images. The Monte Carlo (MC) technique is considered one of the best candidates for this task owing to its ability to comprehensively model the propagation of protons and the subsequent by-products (secondary particles) resulting from proton interactions in the medium. MC simulation is a very comprehensive tool for evaluating proton beam quality or verifying treatment planning systems (TPS). Monte Carlo N-Particles Transport Code, Extension (MCNPX) and Geometry and Track, version 4 (GEANT4) are currently the most commonly used MC codes for proton therapy. Many researchers have used MC simulation to construct their virtual proton facilities in different countries.[2-4] Fontenot *et al*. utilized MCNPX to design proton therapy nozzles based on the double scattering foil technique.[5] Aso *et al*. used GEANT4 to construct particle therapy facilities in the National Cancer Center, East, Hyogo Ion Beam Medical Center, and the University of California San Francisco Medical Center.[6] Shih *et al*. also used GEANT4 to construct particle therapy facilities in the National Cancer Center, Korea,[7] while Cirrone *et al*. built their own particle therapy facility in Italy.[8] Although the CGMH proton facility is not yet ready, Wu *et al*. have presented GEANT4 results about the effect of material composition on proton depth dose distribution.[9] Lee *et al*. published another paper on the MCNPX simulation of proton dose distribution in CT phantoms.[10]

The physics modules used in the GEANT4 and MCNPX are quite different. In GEANT4, the default physics list was chosen so that the standard electromagnetic (EM) process, hadron elastic process, and hadron inelastic process were used. In such a physics list, G4EmStandardPhysics_option3 was implemented for modelling EM process, G4HadronElasticPhysics for elastic process of hadrons, G4HadronPhysicsFTF_BIC for inelastic process of hadrons, G4StoppingPhysics for stopping physics, G4RadioactiveDecayPhysics for radioactive decay, and G4IonBinaryCascadePhysics for inelastic process. The Quark-Gluon String Precompound model was implemented to handle collision of high energy hadrons; the Laboratory for High Energy Physics model was used for sampling elastic scattering between particles except pions; and the Binary cascade model was used for inelastic process of hadrons.[11] In contrast, MCNPX mostly used tabulated cross sections if available. Tabulated cross sections covers neutron physics (0–150 MeV), photon (1 keV–10^5 MeV), electron (1 keV–1000 MeV), and proton (1 keV–150 MeV, where there is only dE/dx data for 1 keV–1 MeV). MCNPX standard elastic scattering model was based on HERMES, a MC code for ultra-high energy cosmic rays above 10^{18} eV. Preequilibrium model was implemented following Bertini intranuclear cascade equilibrium model; Rutherford Appleton Laboratory fission-evaporation model was implemented for radioactive decay; and Fermi breakup model was used for the disintegration of light nuclei.[2]

In this study, a dose simulation system was constructed based on the MCNPX package in order to simulate proton dose distribution in a water phantom. Furthermore, multiple Coulomb scattering (MCS) has been extensively studied in the literature.[12] The subcentimetre lateral dose distribution will significantly impact on MC transport owing to proton disequilibrium and multiple scattering, predominantly because the full width half maximum (FWHM) of proton scattering inside water is in the order of a few millimetres. The simulation of proton transport under these conditions has to be carefully studied in order to obtain accurate results.[13] Comparisons of MC simulations and the pencil beam algorithm may help to clarify dose distribution under proton disequilibrium, which is likely to occur in lung dosimetry. The subcentimetre lateral dose distribution was also studied to understand the dose deviation between different MC simulations and the pencil beam algorithm.

METHODS

In this study, the MCNPX code was selected to model the transport and interactions of particles in the phantom. MCNPX is a modern, general-purpose MC radiation transport computer code that is capable of tracking 34 particle types at nearly all energies (from few keV to TeV). It uses the continuous energy cross section data from the Evaluated Nuclear Data Files, version B-6 libraries and facilitates a variety of source distributions, detector conditions, and user-configurable output options.[14] MCNPX are written with user-friendly interfaces that require minimal modification of the source code. The user only needs to write an input file including the incident proton, phantom geometry, and scoring tallies for the MCNPX code to simulate proton dose distribution inside a phantom.

MCNPX treats proton interactions above 150 MeV (20 MeV for some materials without cross section data of 20–150 MeV) with physical models, such as the Bertini and Isabel cascade models combined with multistage preequilibrium models and evaporation models.[2,15,16] For energies

below 20 MeV, MCNPX relies on Monte Carlo N-Particles Transport Code (MCNP) to complete the low-energy part of the neutron and photon transport.[17] Combining the general features of MCNP with the theoretical models of Los Alamos High-Energy Transport, MCNPX can handle the transport and interaction of neutrons, photons, electrons, protons, and heavy charged particles over a wide range of energies.[2]

A phantom is essentially an array of three-dimensional voxels (volume elements), which can be implemented into MCNPX using its built-in "repeated structures" feature. "Lattices" are used in MCNPX to fill cells of repeated structure, and "Universes" are the element which can be filled into the lattices. A unique "Universe" number is assigned to every material in the phantom to designate material properties such as density and elemental composition. All of these voxels will be joined within a matrix of "Lattices" to assemble the whole phantom. MCNPX was applied in this study using the feature ''mesh tally'' to facilitate the calculations, where the dose mapping of a large number of tallies was necessary. The mesh tally is the most accurate option in MCNPX for handling large numbers of tallies in a volume.[18,19] This option is the fastest and provides the smallest output for convenient importation into other databases or programs. Tallying is the process of scoring the MCNPX results. Each tally option is defined by an Fn command, where n is a unique number. For instance, the F5 tally calculates the flux at a point rather than averaged over a cell. This flux can then be converted into a point dose. On the other hand, the kerma in a cell can be explicitly calculated using the F6 tally, whereas the F8 tally calculates the deposited energy in a cell and can be converted to the cell dose. In this study, the mesh tally was applied to calculate the proton dose distribution inside a water phantom. The mesh tally employs a virtual grid structure that is superimposed on the geometry, rather than being defined as part of the geometry, in order to estimate the track length distributed in a defined cell.

Two different scenarios were studied, including one proton equilibrium case and one proton disequilibrium case. The doses contributed by different types of particles were studied for the proton equilibrium case. A 160 MeV proton pencil beam was perpendicularly incident into a 40 cm × 40 cm × 50 cm water phantom with a scoring voxel size of 20 cm × 20 cm × 0.2 cm. Energy deposition and fluence were calculated from MCNPX with two different modes: (1) Proton only; and (2) proton and secondary particles, such as photon (p), proton (h), electron (e), neutron (n), helium-4 (a), helium-3 (s), triton (t), deuteron (d), and pion (z). The impacts of different MCS models were studied for the proton disequilibrium case. A 70 MeV proton pencil beam was perpendicularly incident into a 40 cm × 40 cm × 10 cm water phantom; two scoring voxel sizes of 0.1 cm × 0.1 cm × 0.05 cm and 0.01 cm × 0.01 cm × 0.05 cm were used for depth dose distribution, and 0.01 cm × 0.01 cm × 0.05 cm for lateral profile distribution simulations.

RESULTS

Dose contribution of different kinds of particles

The incident proton in the material generates many kinds of secondary particles after the collision, such as photons, neutrons, electrons, etc. In MCNPX 2.7.0, the tracking of these secondary particles can be turned on or off. If the tracking of any specific particle is turned off, its kinetic energy will be deposited locally. Such an option can speed up the efficiency of proton simulation; however, it is possible to generate unwanted dose bias in this way.

Figure 1 shows the depth dose curves obtained from MCNPX with two different modes: (1) Proton only (red symbol), where only the proton is simulated; and (2) all particles (blue symbol), where protons and secondary particles are all simulated. The secondary particles resulting from proton interactions with matter include photon (p), proton (h), electron (e), neutron (n), helium-4 (a), helium-3 (s), triton (t), deuteron (d), and pion (z). The symbols inside the parentheses are the official terms used in MCNPX. Although different modes of physics were simulated, it is almost impossible to distinguish between these two curves. There were only minor differences after the Bragg peak. For the proton only simulation, there was no energy deposition beyond its continuous slowing down

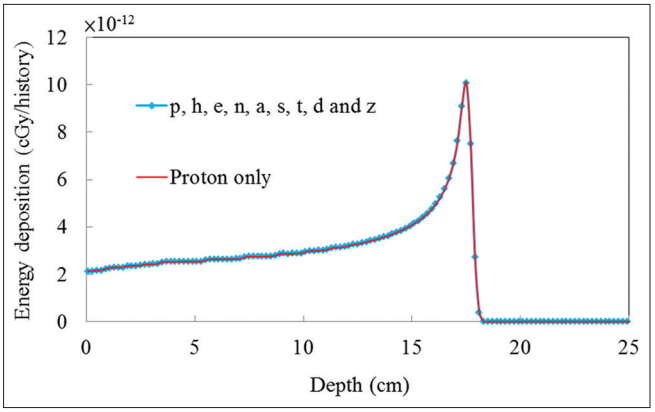

Figure 1: Depth dose curves obtained from MCNPX (1) proton only; and (2) protons and secondary particles including photon (p), proton (h), electron (e), neutron (n), helium-4 (a), helium-3 (s), triton (t), deuteron (d), and pion (z).

approximation (CSDA) range. For the full simulation, including all of the secondary particles listed above, there was a small amount of energy deposition (about 0.1% of the entrance dose) contributed by the secondary particles. In addition, for the computing time comparison, the proton only simulation took 69.11 min, whereas the full simulation took about 163.24 min in a four core AMD Phenom II X4 955 computer with a 64-bit Fedora Core 8 operating system installed. These comparisons suggest that, for radiation therapy purposes, the proton only simulation is optimal for both accuracy and efficiency because secondary particles only contributed about 0.1% of the dose but their simulation consumes about 60% of the computing time. For radiation safety purposes, however, full simulation may be required because 0.1% of the prescribed dose (about 10 mGy) may still be a safety concern for the public, not to mention that these secondary particles may be highly penetrating or of high relative biological effectiveness (RBE). To be noted, the dose reported in this study is absorbed dose, not RBE dose.

Further investigation can be conducted in the analysis of fluences and energy depositions of different particles separately. Figure 2 shows the fluence curves of different particles obtained from MCNPX for 160 MeV protons in a water phantom. The proton contributed almost all of the fluence before its CSDA range was reached. The fluences of neutron and photon were about one order smaller than protons, and the fluences of electrons and deuterons were only about 0.1% of the total fluence. Although it was simulated, the pion contributed no fluence for proton secondary particles in the therapeutic energy range because the pion production threshold in nucleon-nucleon reactions is at 280 MeV.[20]

Figure 3 shows the energy deposition curves of different particles obtained from MCNPX for 160 MeV protons in a water phantom. Although the fluences of neutrons and photons were only one order smaller than that of protons, their contributed dose was about 0.1–1% of the proton dose. The reason for such a low dose contribution is due to their low cross section with water. Protons may have hundreds of thousands of interactions in water, whereas photons and neutrons may only have a few interactions at the same energy. Heliums and deuterons were the second highest contributors to dose besides protons; however, their dose contribution is at most 1–2% of the total dose before the Bragg peak. After the Bragg peak, neutrons and secondary protons become dominant with regard to the dose contribution. This again explains why the proton only mode underestimates the dose after the Bragg peak.

Further, Figure 4 shows the fluence and energy deposition curves of different particles obtained from MCNPX and GEANT4 for 160 MeV protons in a water phantom. In this comparison, the results revealed that although the energy deposition results were almost the same, there were some obvious deviation between the fluence of neutrons simulated using MCNPX and GEANT4. It is difficult to tell which code is more accurate because the secondary neutron doses cannot be assessed using TPS that is not commissioned for low dose (<0.1% of prescribed dose). Furthermore, secondary neutrons are also difficult to measure because neutrons are indirectly ionizing and interact sparsely. Such a finding can also be checked from the literature.[21,22] Usually, GEANT4 shows a greater secondary neutron yield rate for protons with energy lower than 80 MeV but a lower yield rate than MCNPX for protons higher than 80 MeV. This reflects the difference in the physics modules used in MCNPX and GEANT4. GEANT4 uses the precompound model to handle collisions of high energy hadrons but MCNPX uses intranuclear cascade instead. Theoretically, MCNPX contains high-quality physics and

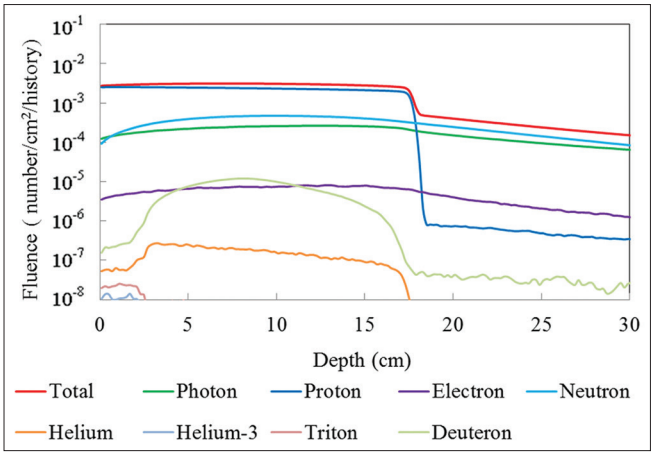

Figure 2: Fluence curves of different particles obtained from MCNPX for 160 MeV protons in a water phantom.

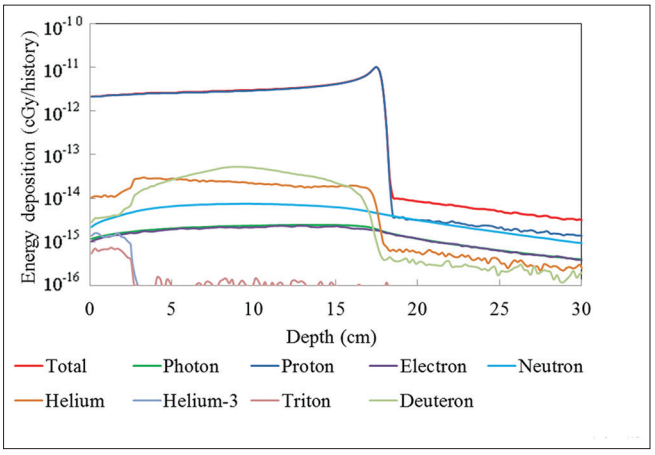

Figure 3: Energy deposition curves of different particles obtained from MCNPX for 160 MeV protons in a water phantom.

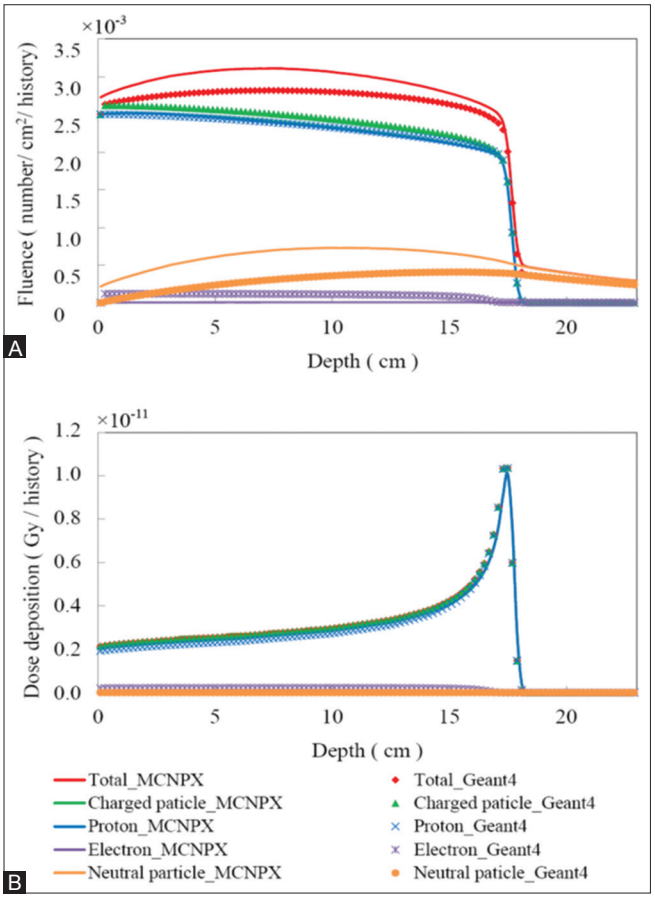

Figure 4: (A) Fluence and (B) energy deposition curves of different particles obtained from MCNPX and GEANT4 for 160 MeV protons in a water phantom.

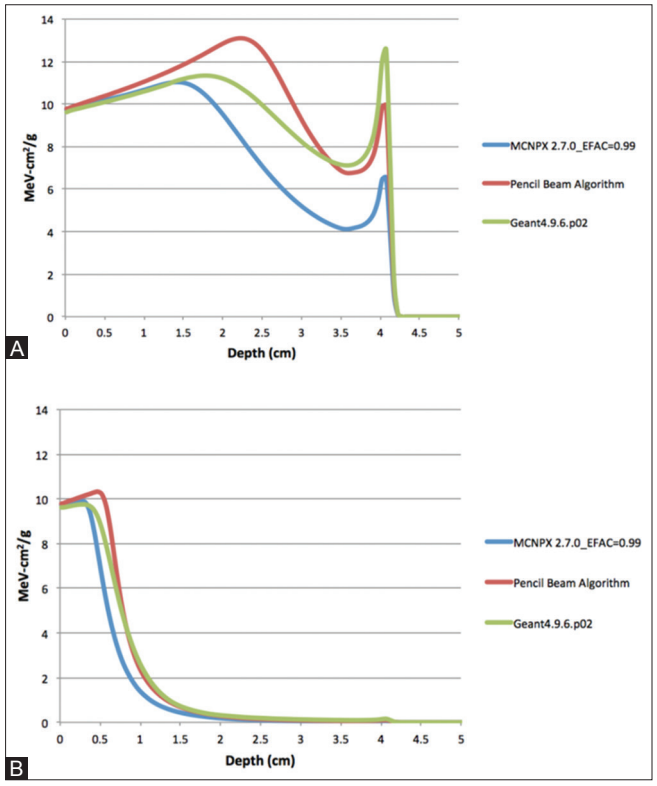

Figure 5: Depth dose distribution in (A) 0.1 cm × 0.1 cm × 0.05 cm and (B) 0.01 cm 0.01 cm 0.05 cm voxels of 70 MeV proton pencil beam in the central axis of a water phantom obtained from MCNPX, GEANT4, and pencil beam algorithm.

has access to the most up-to-date cross-section data which should give more accurate simulation results.

Impacts of different multiple Coulomb scattering models

Figure 5 shows the depth dose distributions of a 70 MeV proton pencil beam in a water phantom obtained from MCNPX, GEANT4, and the pencil beam algorithm in two different scoring voxels, (a) 0.1 cm × 0.1 cm × 0.05 cm and (b) 0.01 cm × 0.01 cm × 0.05 cm. The MCNPX results were simulated using MCNPX 2.7.0 with an EFAC =0.99 setup, which means that the energy loss per energy step was at most 1%. The GEANT4 results were simulated using GEANT4 version 4.9.6.p02. The pencil beam algorithm was developed according to Hong's algorithm.[23] In such small voxels, depth dose distribution is very sensitive to the voxel size. In Figure 5A, the MCNPX and GEANT4 results show a significant deviation of up to 43% at the depth around 35 mm when the voxel size is 0.1 cm × 0.1 cm × 0.05 cm. The reason why the dose deviation is more significant in Figure 5A is that the lateral spread owing to MCS models in water is about 0.1 cm which is very close to the size of voxels and a tiny variation of MCS models could cause significant dose deviation. This deviation, however, was significantly reduced when the voxel size was reduced into 0.01 cm × 0.01 cm × 0.05 cm, as shown in Figure 5B. Also, both MCNPX and GEANT4 results deviated from the pencil beam algorithm significantly. The reason for this deviation is mainly caused by the modelling of MCS.[13] Hong's algorithm only used one simple Gaussian to model the scattering angle distribution, while both MCNPX and GEANT4 used more complicated assumptions, as shown in Figure 6. MCNPX results had a wider FWHM than those for GEANT4, leading to a lower depth dose on the central axis. Similar findings were reported by Kimstrand *et al*.[13] However, Kimstrand *et al*. also compared experimental data with GEANT4, MCNPX, and FLUKA and concluded that all of these codes underestimated the probability of outscatter. MCS can be accurately modelled only if careful tuning of transport parameters was performed. However, more complete simulations usually consume longer computing times and reduce the MC efficiency.

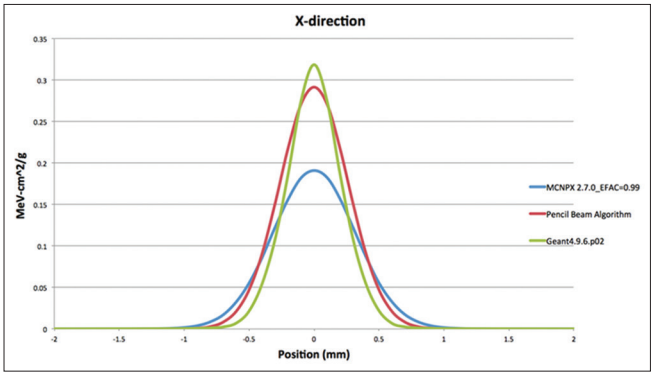

Figure 6: Lateral profile in 0.01 cm × 0.01 cm × 0.05 cm voxels of 70 MeV proton pencil beam in a water phantom (at 2 cm depth) obtained from MCNPX, GEANT4, and pencil beam algorithm.

Conclusions

In the water phantom, proton fluence and dose in the depths beyond the Bragg peak are slightly perturbed by the setup of the physics model and the choice of the simulated particles. The dose from secondary particles is about three orders smaller, but its simulation consumes a significant computing time. This suggests that the simulation of secondary particles may only be necessary for radiation safety issues with regard to proton therapy.

Depth dose distributions of 0.1 cm × 0.1 cm × 0.05 cm voxels of a 70 MeV proton pencil beam in a water phantom obtained from MCNPX, GEANT4, and pencil beam algorithms, showed significant deviations from each other caused by the modelling of MCS. Careful modelling of MCS is necessary when proton disequilibrium exists, and that may be an important issue for lung dosimetry.

Acknowledgments

This work was supported by the National Science Council, Taiwan Project NSC-102-2314-B-182-054/102-2314-B-182 -059-MY2 and by the Chang Gung Research Project CMRPD1C0643/1C0653/1C0663 and CMRPG380833/CIRPD3E0041 for Proton Therapy Basic Research.

Conflicts of interest

There are no conflicts of interest.

REFERENCES

1. Available from: http://www.ptcog.ch/. [Last accessed on 2015 Oct 07].
2. Waters LS. MCNPX User's Manual. Los Alamos; 2002. Available from: http://www.mcnpxlanlgov/opendocs/versions/v230/MCNPX_230_Manualpdf. [Last accesed on 2012 Apr 15].
3. Hendricks JS, McKinney GW, Fensin ML, James MR, Johns RC, Durkee JW, *et al*. MCNPX 2.6. 0 Extensions. New Mexico, US: Los Alamos National Laboratory, LA-UR-08-2216; 2008.
4. Allison J, Amako K, Apostolakis J, Araujo H, Dubois PA, Asai M, *et al*. Geant4 developments and applications. IEEE Trans Nucl Sci 2006;53:270-8.
5. Fontenot JD, Newhauser WD, Titt U. Design tools for proton therapy nozzles based on the double-scattering foil technique. Radiat Prot Dosimetry 2005;116 (1-4 Pt 2):211-5.
6. Aso T, Kimura A, Kameoka S, Murakami K, Sasaki T, Yamashita T. GEANT4 Based Simulation Framework for Particle Therapy System. In Nuclear Science Symposium Conference Record, 2007 NSS'07 IEEE: 2007. IEEE; 2007. p. 2564-7.
7. Shih J, Kwak J, Kim D, Ahn S, Lim Y, Park S, *et al*. Development of a Monte Carlo Simulation for the Proton Therapy in National Cancer Center, Korea. In 13th Geant4 Collaboration Workshop and Users'Conference: 2008; Kobe, Japan; 2008.
8. Cirrone GA, Cuttone G, Guatelli S, Lo Nigro S, Mascialino B, Pia MG, *et al*. Implementation of a new Monte Carlo – GEANT4 simulation tool for the development of a proton therapy beam line and verification of the related dose distributions. IEEE Trans Nucl Sci 2005;52:262-5.
9. Wu SW, Tung CJ, Lee CC, Fan KH, Huang HC, Chao TC. Impact of the material composition on proton range variation – A Monte Carlo study. Radiat Phys and Chem 2014;104;389–92.
10. Lee CC, Lee YJ, Tung CJ, Cheng HW, Chao TC. MCNPX simulation of proton dose distribution in homogeneous and CT phantoms. Radiat Phys Chem 2014;95:302-4.
11. GEANT4 Physics Reference Manual, Dec, 2009. Available from: http://www.geant4.cern.ch/support/userdocuments.shtml. [Last accesed on 2014 Mar 24].
12. Kawrakow I, Bielajew AF. On the condensed history technique for electron transport. Nucl Instrum Methods Phys Res B 1998;142:253-80.
13. Kimstrand P, Tilly N, Ahnesjö A, Traneus E. Experimental test of Monte Carlo proton transport at grazing incidence in GEANT4, FLUKA and MCNPX. Phys Med Biol 2008;53:1115-29.
14. Rose P. ENDF-201: ENDF/B-VI Summary Documentation. Upton, New York, United States: Brookhaven National Lab; 1991.
15. Bertini HW. Intranuclear-cascade calculation of the secondary nucleon spectra from nucleon-nucleus interactions in the energy range 340 to 2900 MeV and comparisons with experiment. Phys Rev 1969;188:1711.
16. Yariv Y, Fraenkel Z. Intranuclear cascade calculation of high-energy heavy-ion interactions. Phys Rev C 1979;20:2227.
17. Briesmeister JF. MCNP – A General Monte Carlo Code for Neutron and Photon Transport. New Mexico, US: Los Alamos National Laboratory, LA-13709, 1986.
18. Doron O, Wielopolski L, Biegalski S. Advantages of mesh tallying in MCNP5 for soil analysis calculations. J Radioanal Nucl Chem 2008;276:183-6.
19. Yu PC, Chao TC, Lee CC, Wu CJ, Tung CJ. A Monte Carlo dosimetry study using Henschke applicator for cervical brachytherapy. Nucl Instrum Methods A 2010;619:411-4.

20. Norbury JW. Pion production data needed for space radiation. Methods 2009;267:1115.

21. Lei F, Truscott P, Dyer C, Quaghebeur B, Heynderickx D, Nieminen P, *et al*. MULASSIS: A Geant4-based multilayered shielding simulation tool. Nucl Sci IEEE Trans 2002;49:2788-93.

22. Krylov A, Paraipan M, Sobolevsky N, Timoshenko G, Tretyakov V. GEANT4, MCNPX, and SHIELD code comparison concerning relativistic heavy ion interaction with matter. Phys Part Nuclei Lett 2014;11:549-51.

23. Hong L, Goitein M, Bucciolini M, Comiskey R, Gottschalk B, Rosenthal S, *et al*. A pencil beam algorithm for proton dose calculations. Phys Med Biol 1996;41:1305-30.